CMLS, Cell. Mol. Life Sci. 61 (2004) 192–208
1420-682X/04/020192-17
DOI 10.1007/s00018-003-3206-5


CMLS Cellular and Molecular Life Sciences

# Review

# Diversity of structures and properties among catalases

**P. Chelikani[a], I. Fita[b] and P. C. Loewen[a,*]**

[a] Department of Microbiology, University of Manitoba, Winnipeg MB, R3T 2N2 (Canada), Fax: +1 204 474 7603, e-mail: peter_loewen@umanitoba.ca
[b] Institut de Biología Molecular de Barcelona, Consejo Superior de Investigaciones Científicas, 18–26 Jordi-Girona, Barcelona (Spain)

Received 2 June 2003; received after revision 24 June 2003; accepted 1 July 2003

**Abstract.** More than 300 catalase sequences are now available, divided among monofunctional catalases (> 225), bifunctional catalase-peroxidases (> 50) and manganese-containing catalases (> 25). When combined with the recent appearance of crystal structures from at least two representatives from each of these groups (nine from the monofunctional catalases), valuable insights into the catalatic reaction mechanism in its various forms and into catalase evolution have been gained. The structures have revealed an unusually large number of modifications unique to catalases, a result of interacting with reactive oxygen species. Biochemical and physiological characterization of catalases from many different organisms has revealed a surprisingly wide range of catalatic efficiencies, despite similar sequences. Catalase gene expression in micro-organisms generally is controlled either by sensors of reactive oxygen species or by growth phase regulons, although the detailed mechanisms vary considerably.

**Key words.** Catalase; peroxidase; crystal structure; heme; dimanganese.

## Introduction

Catalases, or more correctly, hydroperoxidases, are one of the most studied classes of enzymes. The name catalase was first applied, perhaps inappropriately by today's standards, in 1900 [1], and the protein has been the object of study in many different organisms ever since. The ubiquity of the enzyme, its ease of assay, involving a cheap, readily available substrate, $H_2O_2$, and the spectacular display of oxygen evolution have combined to make it an attractive target for biochemists and molecular biologists alike. A number of reviews of catalases have appeared over the years, and the most recent [2, 3] provide a thorough background of structural and physiological information up to early 2000. There has been no slowing in the appearance of work relevant to catalase physiology and structure, and the focus of this review will be on developments since 2000. Recent insights into the structure of catalases arising from a number of new and informative crystal structures will be presented and discussed in light of implications for the catalytic mechanism. The structural and mechanistic picture will be supplemented with an overview of recent reports on the regulation of expression of catalases.

The overall reaction catalyzed by catalases is the degradation of two molecules of hydrogen peroxide to water and oxygen (reaction 1).

$$2H_2O_2 \rightarrow 2H_2O + O_2 \quad (1)$$

This deceptively simple overall reaction can be broken down into two stages, but what is involved in each of the stages depends on the type of catalase. The mechanism relevant to a particular catalase will be addressed in the appropriate section.

* Corresponding author.

Three classes of proteins unrelated on the basis of sequence and structure exhibit significant catalase activity. The class that is most widespread in nature and which has been most extensively characterized is composed of monofunctional, heme-containing enzymes subdivided based on having large (> 75 kDa) or small (< 60 kDa) subunits. Phylogenetic analyses have demonstrated the existence of two distinct clades or subgroupings of small subunit enzymes and one clade of large subunit enzymes among the monofunctional catalases [4]. The second, less widespread class is composed of bifunctional, heme-containing catalase-peroxidases that are closely related by sequence and structure to plant peroxidases. The third class includes the nonheme or Mn-containing catalases. In addition, a diverse group of proteins, all heme-containing, such as chloroperoxidase, plant peroxidases and myoglobin, exhibit very low levels of catalase activity, attributable to the presence of heme, which alone exhibits catalatic activity [2].

## Regulation of catalase gene expression

Cells usually modulate their stress response systems through regulatory proteins that sense the stressor or a messenger of the stressor and cause appropriate changes in transcription and, occasionally, translation or proteolysis. Most bacteria produce one or more catalases that usually respond to oxidative stress, either directly to $H_2O_2$ levels or to the presence of other active oxygen species. The earliest studies of catalase gene regulation were carried out in *Escherichia coli,* and these have been extensively reviewed [5]. The catalase-peroxidase HPI (hydroperoxidase I), or KatG, is controlled as part of the OxyR regulon, which senses active oxygen species, and the monofunctional catalase HPII is controlled as part of the $\sigma^S$ regulon in stationary phase. Very recently, polyamines, including putrescine, spermidine and spermine, were reported to up-regulate both the *oxyR* and *rpoS* regulons in *E. coli* [6], but the mechanism remains unclear. The commonality of a reactive oxygen sensor and growth phase or $\sigma$-transcription factor control mechanisms in catalase gene expression is illustrated in table 1, although there is no consistency in type of catalase or type of regulator. In addition, other regulators have been adapted to modulate catalase levels, but the generality of their involvement and the regulatory protein involved has not been defined.

Heme synthesis must be sufficiently rapid to satisfy induced catalase synthesis rates. *E. coli* successfully increases the rate of heme synthesis to satisfy the demands for it in cells expressing plasmid-encoded catalases, but whether this is simply a response to heme demand or coordinate regulation of heme operons is not clear. In *Staphylococcus aureus*, *Pseudomonas aeruginosa* and *Bacillus subtilis*, there is coordinate control of oxidative stress proteins and iron storage and transport proteins [7–9], but no link to the control of protoporphyrin synthesis has been demonstrated. There has been one report of iron-deficient catalase from *Proteus mirabilis* (PMC) being produced in *E. coli* during its rapid expression under the control of an inducible T7 promoter [10]. In this instance, presumably the protophorphyrin was available for protein folding, but the availability or insertion rate of iron was limiting.

## Monofunctional, heme-containing catalases

Heme-containing catalases all have in common a two-stage mechanism for the degradation of $H_2O_2$. In the first step, one hydrogen peroxide molecule oxidizes the heme (in heme-containing catalases) to an oxyferryl species in which one oxidation equivalent is removed from the iron and one from the porphyrin ring to generate a porphyrin cation radical (reaction 2).

$$\text{Enz (Por-Fe}^{III}\text{)} + H_2O_2 \rightarrow \text{Cpd I (Por}^{+\cdot}\text{-Fe}^{IV}\text{= O)} + H_2O \quad (2)$$

The second hydrogen peroxide molecule is utilized as a reductant of compound I to regenerate the resting-state enzyme, water and oxygen (reaction 3).

$$\text{Cpd I (Por}^{+\cdot}\text{-Fe}^{IV}\text{= O)} + H_2O_2 \rightarrow \text{Enz (Por-Fe}^{III}\text{)} + H_2O + O_2 \quad (3)$$

Despite this common reaction, there are great differences in reactive capability among the members of this very large family of enzymes, and recent research is only just beginning to provide us with clues that point to some explanations for the differences.

## Phylogeny

Three reviews of catalase phylogeny have appeared, each succeeding review involving an increased number of sequences, from 20 in 1993 [11] to 74 in 1997 [4] to 256 in 2003 [12]. In 1997, the clear division of monofunctional catalases into three clades was obvious, arising from a minimum of two gene duplication events. The more exhaustive recent analysis confirms these conclusions but integrates a larger picture including catalase-peroxidases and nonheme catalases into a universal tree of life. Clade 1 catalases are predominantly of plant origin, but with one algal representative and a subgroup of bacterial origin. Clade 2 enzymes are all large subunit enzymes of bacterial and fungal origin. The one archaebacterial clade 2 enzyme is postulated to have arisen in a horizontal transfer event from a *Bacillus* species. The clade 3 enzymes are all small subunit enzymes from bacteria, archaebacteria, fungi and other eukaryotes. It is

Table 1. Regulatory responses of catalases and catalase-peroxidases in bacteria and fungi.

| Organism | Catalase | Type[a] | Regulator | Additional response | Reference |
|---|---|---|---|---|---|
| *Agrobacterium tumefaciens* | KatA | CPx | OxyR | | [76] |
| *Emericella nidulans* | CatA | 3 | | post-transcriptional control | [77] |
| *Emericella nidulans* | CatB | 2 | | developmental, $H_2O_2$ | [78] |
| *Emericella nidulans* | CatC | 3 | | stationary phase | [79] |
| *Emericella nidulans* | CpeA | CPx | StuA | | [80] |
| *Apergillus niger* | CatR | 2 | | $H_2O_2$ | [81] |
| *Bacillus firmus* | CatII | 3 | | $H_2O_2$/ascorbate | [82] |
| *Bacillus firmus* | CatIII | 2 | | stationary phase | [82] |
| *Bacillus subtilis* | KatA | 3 | PerR | | [83, 84] |
| *Bacillus subtilis* | KatE | 2 | $\sigma^B$ | | [85] |
| *Bacillus subtilis* | KatX | 1 | $\sigma^F$ | | [86] |
| *Bacteroides fragilis* | KatB | 3 | OxyR | | [87] |
| *Brucella abortus* | KatE | 3 | OxyR | | [88] |
| *Dinococcus radiodurans* | CatE | 2 | | $H_2O_2$ | [89] |
| *Escherichia coli* | HPI (KatG) | CPx | OxyR | | [90] |
| *Escherichia coli* | HPII (KatE) | 2 | $\sigma^S$ | | [91] |
| *Haemophilus influenzae* | HktE | 3 | | $H_2O_2$ /ascorbate | [92] |
| *Helicobacter pylori* | KatA | 3 | Fur | | [93, 94] |
| *Mycobacterium smegmatis* | KatG | CPx | FurA | | [95] |
| *Mycobacterium tuberculosis* | KatG | CPx | FurA | | [96] |
| *Neisseria gonorrhea* | Kat | 3 | OxyR | | [97] |
| *Erinea carotovora* | HPII | 2 | $\sigma^S$ | | [98] |
| *Pseudomonas aeruginosa* | KatA | 3 | Fur | | [99] |
| *Pseudomonas aeruginosa* | KatB | 1 | OxyR | | [100] |
| *Pseudomonas putida* | CatA | 3 | | log phase | [101] |
| *Pseudomonas putida* | CatC | 2 | | stationary phase | [101] |
| *Pseudomonas syringae* | CatF | 1 | | stationary phase | [102] |
| *Pyrobaculum calidifontis* | Kat pc | Mn | | aerobic conditions | [103] |
| *Rhizobium etli* | KatG | CPx | OxyR | | [104] |
| *Salmonella typhimurium* | KatM | Mn | $\sigma^S$ | | [105] |
| *Salmonella typhimurium* | HPI | CPx | OxyR | | [106] |
| *Salmonella typhimurium* | HPII | 2 | $\sigma^S$ | | [107] |
| *Sinorhizobium leguminosarum* | Cat | | | log phase | [108] |
| *Sinorhizobium meliloti* | KatA | 3 | | $H_2O_2$ | [109] |
| *Sinorhizobium meliloti* | KatC | 2 | | stationary phase | [110] |
| *Staphylococcus simulans* | ACKI | | | oxygen | [111] |
| *Staphylococcus aureus* | KatA | 3 | PerR, Fur | | [7, 112] |
| *Streptomyces coelicolor* | CatA | 3 | CatR | | [113] |
| *Streptomyces coelicolor* | CatB | 2 | $\sigma^B$ | | [114] |
| *Streptomyces coelicolor* | CatC | CPx | FurA | | [115] |
| *Streptomyces reticuli* | CpeB | CPx | FurS | | [116] |
| *Vibrio fischeri* | KatA | 3 | | stationary phase, $H_2O_2$ | [117] |
| *Xanthomonas oryzae* | KatX | 2 | $\sigma^S$ | | [118] |
| *Xanthomonas campestrisi* | KatE | 2 | $\sigma^S$ | | [119] |

[a] 1, clade 1; 2, clade 2; 3, clade 3; CPx, catalase-peroxidase; Mn, manganese-containing catalase.

postulated that the archtypal monofunctional catalase was a large subunit clade 2 enzyme from which an early gene duplication event, accompanied by loss of the sequence at the 5′ and 3′ ends, gave rise to the clade 1 enzymes. Clade 3 enzymes are not present in older taxonomic groups, suggesting that they arose much later in evolution as a result of a gene duplication in bacteria that then spread by horizontal and lateral transfers among bacteria to archaebacteria and eukaryotes. The division into three clades is illustrated in figure 1 with a focus on the nine catalases for which structures have been determined.

**Kinetic properties**

Many catalases have been characterized over the century of study, but very few of the enzymes have been characterized side by side. This has resulted in many independent reports of activities and properties, but no way to properly compare the results. Such a comparison of 16 common catalases, including seven for which the structures have been determined, has revealed just how great a divergence in properties there is within the catalase family [13]. Catalases do not follow Michaelis-Menten kinetics except at very low substrate concentrations, and different enzymes are affected differently at higher substrate

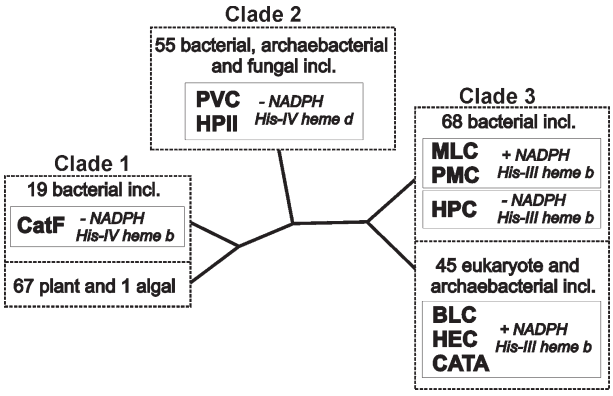


Figure 1. Phylogenetic tree of the monofunctional catalases, focusing on the nine catalases for which structures have been determined. The highlighted enzymes are a subset of the 255 sequences used to generate the tree [12]. Adjacent to each enzyme is a summary of heme type (b or d), heme orientation and whether or not NADPH can bound (+ or –, respectively). The heme can be oriented with the imidazole ring of the essential histidine located either above ring III (His-III) or above ring IV (His-IV) of the heme.

concentrations. Most small subunit enzymes begin to suffer inactivation by $H_2O_2$ at concentrations above 300–500 mM and never reach the Michaelis-Menten $V_{max}$ predicted by extrapolation from rates at low substrate concentrations. On the other hand, large subunit enzymes start to suffer inhibition only above 3 M [$H_2O_2$], if at all, and exceed the predicted Michaelis-Menten $V_{max}$. Consequently, the presentation of observed data in terms of the typical constants $K_m$ and $V_{max}$ is misleading because true Michaelis-Menten kinetics are not applicable. With this proviso in mind, the observed $k_{cat}$ values ranged from 54,000 $s^{-1}$(*P. aeruginosa* KatB) to 833,000 $sec^{-1}$ (PMC), and the [$H_2O_2$] at $V_{max}/2$ ranged from 38 to 599 mM. Sequence differences among catalases must be responsible for the widely differing reaction rates and substrate affinities, but providing a rationale for how is not yet possible. Greater insights into the reaction mechanism must be gained before this goal will be realized.

## Catalases are uniquely stable

The conclusion from phylogenetic reasoning that the archetypal catalase was a clade 2, large subunit enzyme is supported by the unusual resistance to denaturation and proteolysis exhibited by enzymes from this clade. Resistance of catalase HPII to pH and thermal denaturation was noted early in the study of catalases from *E. coli* and other enteric bacteria and used as a diagnostic test to differentiate among catalases in crude extracts [14, 15].

Documentation of the thermal stability revealed that there was actually a small increase in activity above 60 °C and that activity began to drop only above 80 °C, with a $T_m$ of 83 °C [16]. The loss of activity was accompanied by changes in secondary structure, but the dimer association was not affected. Boiling in buffer, or alternatively, heating to 65 °C in 5.6 M urea was required to dissociate the dimer. While not as stable as HPII, small subunit catalases such as bovine liver catalase (BLC) still exhibited enhanced stability for an enzyme from an organism normally growing at 37 °C, with a $T_m$ for loss of activity of 56 °C. The thermal stability of HPII has also been utilized as a purification step [13] . Catalases, generally, are also resistant to treatment with an ethanol:chloroform mixture, another property that can be exploited as a tool for catalase purification [13]. Unfortunately, HPII protein heated above 60 °C or treated with ethanol:chloroform does not readily crystallize, suggesting that some alterations in structure have occurred that were not reflected in enzyme activity.

Another example of the robustness of HPII lies in its retention of high levels of activity even after treatment with a 1:1 (w:w) ratio of proteinase K for 16 h at 37 °C [17]. Despite the retention of activity, a closer analysis revealed that the protein had suffered limited cleavage but that the core of the enzyme containing the heme active site remained intact. Rapid cleavage of about 75 N-terminal residues occurred initially within one h, followed by a slower cleavage of 160 C-terminal residues. Removal of the C-terminal domain exposed one further protease sensitive sight that allowed cleavage of the subunit into two approximately equal-sized fragments. Despite the introduction of this last nick and possibly one other nearby, the monomers remained intact within the larger tetramer.

Both thermal stability and resistance of the majority of the protein to proteolysis can be explained in terms of a very rigid, stable structure that resists unfolding, thereby preventing access to the protease active site. Resistance to proteolysis is an advantage to HPII because it is expressed in stationary phase, a period of rapid protein turnover and elevated protease levels. There would have been a strong selective pressure to retain this property, but it is not clear whether resistance to proteolysis evolved in *E. coli* and thermal stability was an inadvertent outcome. Alternatively, the catalase could have originated in a thermophilic organism and been horizontally transferred to *E. coli,* where protease resistance has been the selective pressure for retention of thermal resistance.

The enhanced thermal stability of HPII was initially ascribed to the extended sequence of 80 residues from one subunit being overlapped by the wrapping domain of an adjacent subunit [16]. However, proteolytic removal of all but 5 residues of the overlapped N-terminal region did not significantly affect the thermal stability, whereas removal of the C-terminal domain lowered the $T_m$ by more than 25 °C [17]. The importance of the N-terminal sequence in folding and oligomerization was demonstrated in HPII variants, N-terminally truncated by only 20 residues, not accumulating protein when expressed from mutant genes [18], and this has been confirmed in the

catalase from *Candida tropicalis,* where truncation by 4 or 24 residues produces aggregates of inactive protein smaller than tetrameric [19]. In the latter case, even the 4-residue truncation eliminates the overlap or interweaving feature common to catalases, which would be expected to have an effect on subunit association. Longer truncations extending to within 3 residues of the heme active site had the expected effect of preventing heme binding [19].

## Insights from recent structures

New insights into catalase function have been provided by the solution of two monofunctional catalase structures, one published and the second soon to be reported, and the comparison of the structures of a number of variants with the earlier released native structures [see table 2 for Protein Data Base (PDB) accession numbers]. The previously reported seven catalase structures include the small subunit clade 3 enzymes from BLC [20, 21], *Micrococcus lysodeiticus* (MLC) [22], PMC [23], *Saccharomyces cerevisiae* (CATA) [24, 25], and human erythrocytes (HEC) [26] and the large subunit clade 2 enzymes from *Penicillium vitale* (PVC) [27, 28] and *E. coli* (HPII) [29, 30]. The two new structures include *Pseudomonas syringae* (CatF) [31, 32], which provides the first look at a clade 1 catalase, and the *Helicobacter pylori* catalase (HPC) with and without formic acid bound [P. C. Loewen et al., unpublished]. The typical core catalase features of a heme-containing active site deeply buried in a beta-barrel structure with two or three channels providing access to the heme has been described in many papers and reviews. Some of the similarities and differences between small and large subunit catalases are evident in the structures of CatF and HPII in figure 2. The CatF and HPC structures retain these common features, but CatF presents an unexpected heme orientation and lacks reduced nicotinamide adenine dinucleotide phosphate (NADPH). In addition, the presence of four subunits in the asymmetric unit of CatF makes possible an assessment of asymmetry, particularly in solvent location, among subunits and in comparison with other catalases.

## Heme orientation

The first catalase structures solved, BLC and MLC, had a common heme orientation in which the active site His was situated above ring III of the heme (referred to as the His-III orientation), leading to the conclusion that this was the normal orientation for heme in catalases. This was reinforced by the heme orientation found in PMC, CATA and HEC. The presence of the 'flipped' orientation with the active site His located above ring IV of the heme (His-IV) in PVC and HPII was assumed to be unique to large subunit enzymes. The fact that the hemes in PVC and HPII were modified to heme d with a *cis*-hydroxyspirolactone group on ring III [33] reinforced the idea that large subunit enzymes were unique. The CatF structure presents heme in the His-IV orientation, suggesting that the 'normal' and, in view of probable evolutionary development, original orientation of heme in catalases is His-IV. The residues making contact with the two methyl groups and two vinyl groups on rings I and II create a matrix of van der Waals interactions that favor the His-IV orientation in CatF, PVC and HPII and that would prevent any attempt to flip the heme to the His-III orientation. Similarly, the matrix of van der Waals interactions in the clade 3 catalases BLC, MLC, PMC, HEC and CATA favor the His-III orientation and would prevent adoption of the His-IV orientation. A survey of 228 catalase sequences identified residues at the positions equivalent to 301 (Ala) and 350 (Leu) in CatF that are the key determinants in heme orientation through their proximity to

Table 2. Protein Data Bank accession numbers for native catalases, their complexes and variants (available at *www.rcsb.org/pdb*).

| Catalase | Organism | Accession numbers |
|---|---|---|
| A. Monofunctional catalases | | |
| PVC | *Penicillium vitale* | 4CAT |
| BLC | *Bos taurus* (liver) | 7CAT, 8CAT, 4BLC |
| PMC | *Proteus mirabilis* | 2CAG, 2CAH, 1M85, 1MQF, 1E93 |
| CATA | *Saccharomyces cerevisiae* | 1AE4 |
| HEC | *Homo sapiens* (erythrocyte) | 1DGB, 1DGF, 1DGG, 1DGH, 1F4J, 1QQW |
| HPII | *Escherichia coli* | 1GGE, 1IPH, 1CF9, 1GG9, 1GGF, 1GGH, 1GGJ, 1GGK,1QF7, 1P7Y, 1P7Z, 1P80, 1P81, IQWS |
| MLC | *Micrococcus lysodeikticus* | 1GWE, 1HBZ, 1GWF, 1GWH |
| CatF | *Pseudomonas syringae* | 1M7S |
| HPC | *Helicobacter pylori* | 1QWL, 1QWM |
| B. Catalase-peroxidases | | |
| HmCPx | *Haloarcula marismortui* | 1ITK |
| BpKatG | *Burkholderia pseudomallei* | 1MWV |
| C. Manganese catalases | | |
| LPC | *Lactobacillus plantarum* | 1JKU, 1JKV |

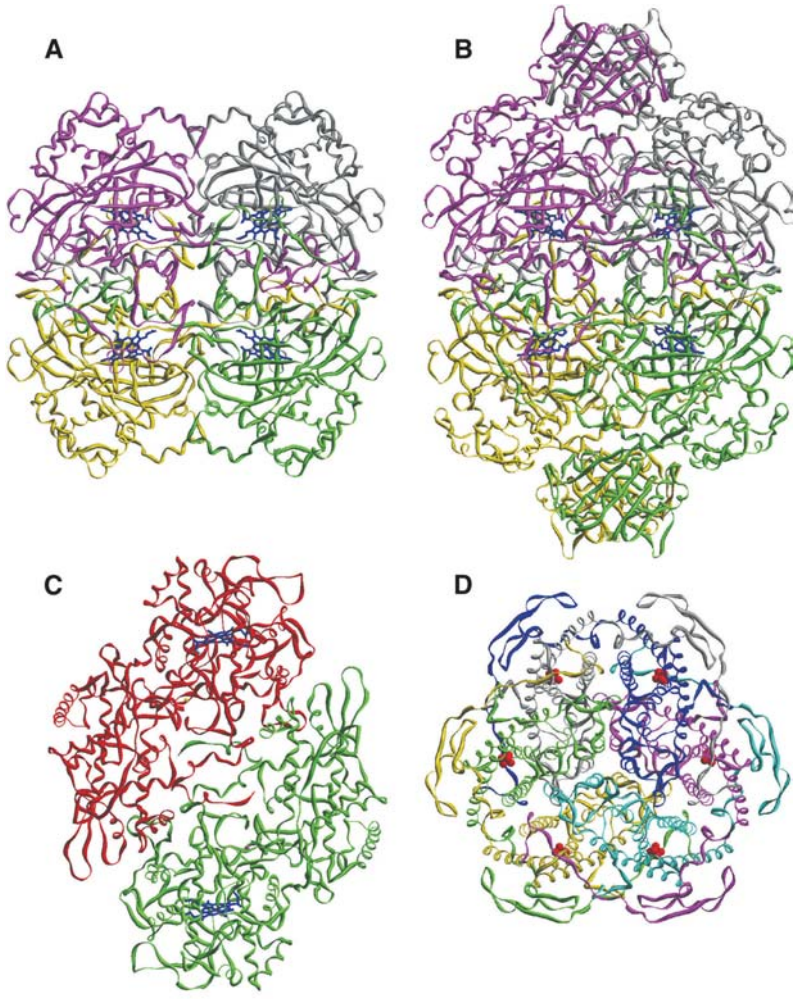


Figure 2. Ribbon diagrams for comparison of the overall structures and sizes of heme-containing small and large subunit catalases, a catalase-peroxidase and a dimanganese catalase. A tetrameric small subunit, heme-containing catalase, CatF (*A*), a tetrameric large subunit, heme-containing catalase, HPII (*B*), a dimeric catalase-peroxidase, BpKatG (*C*) and a hexameric dimanganese catalase, LPC (*D*), are presented. The structures in *A* and *B* are both viewed looking down the Q axis to facilitate comparison of the structures, in particular of the added C-terminal domains in HPII. In *C*, BpKatG is viewed along the noncrystallographic two-fold symmetry axis. All structures are presented in the same scale. The dimensions of the four structures (X by Y) are 93 Å × 93 Å for CatF (*A*), 85 Å × 136 Å for HPII (*B*), 83 Å × 108 Å for BpKatG (*C*) and 90 Å × 81 Å for LPC (*D*). The hemes are shown in *A, B* and *C* in blue, and the dimanganese clusters in *D* are shown in red. The figure was prepared using SETOR [120].

the vinyl groups on rings I and II. At position 301, 0% of clade 1 and clade 2 enzymes have Leu or Ile, but 80% of clade 3 enzymes do. The larger group prevents adoption of the His-IV orientation. At position 350, 69% of clade 1 enzymes and 100% of clade 2 enzymes have Leu, whereas 0% of clade 3 enzymes do, and the location of the Leu side chain prevents adoption of the His-III orientation. The recently solved structure of HPC conforms to this rule in presenting the His-III orientation. Occupancy at the equivalent position in other catalases suggests that most clade 1 and all clade 2 enzymes will have the His-IV orientation and that most clade 3 enzymes will have the His-III orientation. It will be interesting to determine whether the apparent sequence exceptions conform to the clade majority, whether there is a mixture of heme orientations or whether there are small subsets of clade 1 and clade 3 enzymes with His-III and His-IV orientations, respectively.

## NADPH binding

Since it was first noted almost 20 years ago [34], the presence of NADPH in catalases has presented the interesting problem to biochemists of explaining the purpose of the cofactor, and of determining its universality. The structures of the clade 3 enzymes BLC, HEC, PMC and CATA all contain NADPH in some fraction of their subunits, whereas the cofactor is not evident in the structures of the clade 2 enzymes PVC and HPII. NADPH is not evident in the structure of CatF, and the potential binding site is

modified compared with clade 3 binding sites to such an extent that NADPH binding should not be possible. The NADPH binding pockets of BLC, HEC, CATA and PMC contain a His, an Arg, a Val and a His (193, 202, 301 and 304, respectively, using BLC numbering), which may be considered to be signatures for NADPH binding. In CatF, the equivalent residues are $Arg_{196}$, $Glu_{205}$, $Ile_{304}$ and $Asp_{307}$, each of which would interfere with NADPH binding either through electrostatic repulsion, direct steric interference or loss of favorable contacts. All clade 1 catalases lack the equivalent of $Arg_{202}$ and $His_{304}$, and most lack $His_{193}$ and $Val_{301}$, leading to the conclusion that most, if not all, clade 1 catalases do not bind NADPH. In the case of clade 2 enzymes, a portion of the extended C-terminal sequence protrudes into the NADPH binding site, precluding any possibility of NADPH binding in these enzymes. The conclusion seems to be that only clade 3 enzymes bind NADPH, but even in this clade, the coenzyme is not universal, based on the signature residues, and the structure of HPC confirms this conclusion. A region of electron density that might be assigned to NADPH is not evident in the electron density maps of HPC, and the signature residues are sufficiently changed, including the equivalent of $His_{193}$ to Tyr, $Val_{301}$ to Ile and $His_{304}$ to Thr, to make fitting of NADPH into the site difficult, if not impossible.

The widespread nature of the His-III orientation of heme in clade 3 enzymes suggests that this feature was adopted shortly after the separation of clade 3 from clade 1 enzymes. The more limited nature of NADPH binding among clade 3 enzymes also suggests that it evolved independently and at a later date, arguing against a direct evolutionary link between the His-III orientation of the heme and NADPH binding as previously speculated [32].

The role of NADPH and the presumed reason for its binding site having evolved are to prevent the formation of inactive compound II [34], but the mechanism by which this is achieved remains unclear [35–38]. Clade 2 enzymes do not form compound II, or at least it has not been possible to generate compound II in the laboratory, making NADPH binding unnecessary. Similar attempts to generate compound II from a clade 1 catalase have not been reported. Curiously, the electron density maps of HPC suggest that one of the two subunits in the asymmetric unit is in an oxyferryl form and that treatment with formic acid converts the oxyferryl species to an unmodified iron. This is consistent with earlier work showing that formic acid can reduce compound I and promote the conversion of compound II to native state [2]. Given the apparent stability of the oxyferryl species in HPC, it is unlikely that it is either compound I or II, although it is degraded by formic acid treatment. Several electron donors can reduce compound I and II back to the ferric state [2], and it is tempting to speculate that the evolution of NADPH binding in a small subset of catalases may have been the result of these other recovery routes becoming limited, possibly as a result of environmental changes. Based on this very limited experimental picture, one might postulate that compound II recovery was not a problem for the progenitor large subunit catalases. As the early small subunit enzymes evolved, they were either not converted to compound II or the compound II was recovered through the involvement of readily available metabolites such as formic acid, ascorbate and phenols [2]. With the appearance of clade 3 enzymes, which are converted to compound II, and the evolution of more specialized intracellular environments, the availability of reducing metabolites may have become restricted, or the prevalence of NADPH may have increased, allowing catalases in some species to utilize it as the tool for preventing compound II formation.

## Catalase as a source of reactive oxygen species and another role for NADPH

The usual physiological role ascribed to catalases is that of removing $H_2O_2$, a reactive oxygen species (ROS), before it can cause cellular damage. It was therefore surprising to find that catalase in human and mouse keratinocytes is responsible for the generation of ROS upon irradiation with UVB light [39]. The ROS were not identified, but singlet oxygen and superoxide were eliminated, making hydroperoxides the most likely species. This new and very exciting development, the detoxification of UVB light through generation of $H_2O_2$, which is also degraded by the catalase, has been heralded as a second role for catalases.

The mechanism of ROS generation by catalase remains unclear, however. Significantly, normal catalase inhibitors such as azide, aminotriazole and cyanide, which bind to the heme iron and essential imidazole ring, activate the production of ROS. When the effect of inhibitors is considered in the context that the Soret absorbance maximum for heme in the native enzyme is at 407 nm, well removed from the 290 to 320 nm region for UVB light, it seems unlikely that the heme center is actively involved in the generation of ROS, and NADPH, a cofactor of mammalian catalases, may prove to be involved. The wavelength of maximum absorbance for NADPH is 340 nm, and the cofactor is a logical source of the electrons required for reduction of molecular oxygen. Future work involving comparison with catalases that do not bind NADPH should clarify the mechanism of this intriguing property. Furthermore, if the NADPH cofactor is found to have a role in ROS generation, it will suggest another role for NADPH in catalase physiology and a possible explanation for why NADPH binding in catalase evolved.

**Channel architecture**

The recently reported structures of CatF [32] and HPII variants [40] have provided significant insights into the channel architecture in catalases. Three obvious channels connect the heme-containing active site with the surface. The main channel, so named because it is the most obvious access route to the heme, approaches the heme perpendicular to its plane and has long been considered the primary access route for substrate $H_2O_2$, a concept supported by molecular dynamics modeling [41, 42]. A comparison of the main channels in CatF and HPII (fig. 3) reveals the extended and bifurcated structure in HPII as compared with the shorter funnel shape in CatF, which is representative of other small subunit enzymes. A second channel approaches the heme laterally, almost in the plane of the heme, and has been referred to as the minor or lateral channel. Limited evidence pointing to a role for the lateral channel in HPII includes a 3-fold increase in specific activity resulting from an enlargement of the channel through removal of $Arg_{260}$, part of the Glu-Arg ionic pair situated in the channel. A third channel connects the heme with the central cavity, but no evidence of it having a role has been presented.

An extensive review of the waters occupying the main channels in each of the four subunits of CatF, HEC (+ CN and + peracetic acid), CATA + azide and HPII, and of the single subunits of MLC and PMC, revealed a number of consistently occupied positions as well as a number of low occupancy sites [32]. All enzymes contain a water interacting with the catalytic residues His and Asn, and some catalases, including HPII, MLC and PMC, contain a second water in the active site interacting with the heme iron and the active site His. Moving away from the heme in the channel, only one subunit of HPII and all subunits in inactive HEC contain waters in the hydrophobic region around the conserved $Val_{169}$ (HPII numbering). The lack of waters in the hydrophobic portion of the channel between the conserved Asp (12 Å from the heme) and the active site His was interpreted as a 'molecular ruler' effect [26] attributed to the lack of interaction sites on the protein and a distance that was inappropriate for the formation of a stable matrix of hydrogen-bonded waters, but appropriate for a matrix involving the slightly larger $H_2O_2$. While elements of the ruler model may be applicable, the new structures suggest that a more complex series of interactions control substrate access to the active site.

The first point to consider is that a matrix of water can form in the hydrophobic portion of the channel of HEC treated with peracetic acid in the absence of any new constituents or structural changes. Secondly, there seems to be an optimum three-dimensional shape and size for this portion of the channel, because making the channel in CATA or HPII either smaller (V169A in HPII) or larger (V169I in HPII) reduced [25, 40] enzyme-specific activity. Finally, changing the conserved Asp (181 in HPII) to any uncharged residue, polar or nonpolar, including Asn, Gln, Ala, Ser and Ile caused a loss of enzyme activity and a reduction in solvent occupancy in the channel [40]. Most notably, the sixth ligand water was absent in all subunits of D181A, D181S and D181Q variants, and there were generally fewer waters in the channel. By contrast, the D181E variant exhibited normal levels of activity and contained not only the sixth ligand water in all subunits, but an unbroken water matrix extending the full length of the channels.

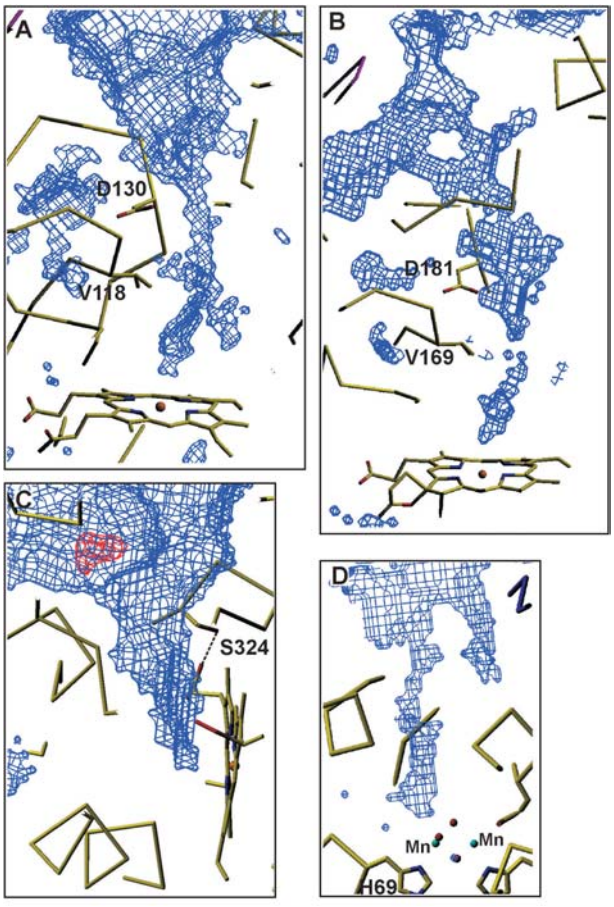


Figure 3. Structure of the channels providing access to the active sites in one subunit each of CatF (*A*), HPII (*B*), BpKatG (*C*) and LPC (*D*). The channel, as calculated by the program VOIDOO [121], is presented as a blue chicken-wire structure in a cross-section slab of the enzyme. In *A* and *B*, the key valine ($V_{118}$ and $V_{169}$) and aspartate residues ($D_{130}$ and $D_{181}$) discussed in the text are indicated. In *C*, the key serine ($S_{324}$) discussed in the text is indicated, and its hydrogen bond with the propionate is indicated by a dashed line. Also in *C*, the region of unassigned electron density corresponding to an INH-like molecule is presented in a red chicken-wire structure. The active site heme is evident at the end of the channels in *A, B* and *C*. In *D*, the dimanganese cluster is presented as two blue balls (Mn) and four red balls (waters), and one of the coordinating histidines (His69) is indicated for reference. All four channels are presented in the same scale for comparison. Note that the approach to the heme in *C* is in the plane of the heme in comparison to the approach perpendicular to the plane of the heme in *A* and *B*. The figure was prepared using SETOR [120].

This striking influence of the negatively charged side chain at position 181 of HPII may lie in the generation of an electrical potential field in the hydrophobic portion of the channel between the negative charge and the positively charged heme iron. The potential field will influence the orientation of any molecule with an electrical dipole, including both water and hydrogen peroxide. In both cases, the preferred orientation will be with oxygen atoms pointed toward the positively charged heme iron and the hydrogens toward the negatively charged side chain of aspartate or glutamate. Such a uniform orientation in the population of solvent will facilitate the formation of hydrogen bonds, providing an explanation for increased water occupancy when Asp or Glu are present at position 181 in HPII. A second result of the induced orientation of hydrogen peroxide is that it will enter the active site with one oxygen oriented toward the heme iron, the hydrogen on this oxygen located within hydrogen-bonding distance of the essential His and the second oxygen situated within hydrogen-bonding distance of the $NH_2$ of the active site Asn. This perfectly explains the suggestion arising from molecular dynamics studies that the substrate hydrogen peroxide enters the active site in a preferred orientation. Further support for the involvement of a potential field is provided by the structures of CatF, PMC and HEC [32], which reveal an increasingly weaker interaction between the heme iron and the sixth ligand water. The heme propionate in each case forms a hydrogen bond with either a Gln (CatF), a His-His complex (PMC) or a His-Asp-Tyr complex HEC. As the likelihood for electron transfer into the heme ring increases, thereby decreasing the effective positive charge on the heme iron, the association of water with the heme iron decreases. Despite this apparent correlation between weaker dissociation at the heme and inductive effects, the situation is clearly more complex because HEC exhibits one of the fastest turnover rates. Finally, it is conceivable that the electrical potential field might serve to polarize electrons in the hydrogen peroxide, facilitating formation of the transition state.

The folding of catalases has proven to be very sensitive to minor disruptions in structure within the active site. For example, the active site variants of HPII, H128A and H128N folded properly and protein accumulated, but the variants H128E and H128Q did not accumulate any protein despite the presence of sufficient room to accommodate the longer side chain [43]. Given the central position of heme in catalase structure, the isolation and characterization of an iron-deficient PMC was a surprise. PMC expressed from a gene under the control of a T7 promoter was found to lack iron in about 70% of the molecules, presumably because the rapidly produced protein sequestered the protoporphyrin faster than iron could be inserted [10]. Despite the lack of iron, there is very little distortion in the heme or in the protein surrounding the heme. Even the proximal tyrosine, which normally associates with the heme iron, is shifted very little, remaining associated with the pyrrole nitrogens. Not surprisingly, the iron-deficient protein is less active in proportion to the loss of iron.

## Catalase-peroxidases

Despite a very different sequence and tertiary/quaternary structure, the overall catalatic reaction of catalase-peroxidases takes place via the same two stages (reactions 2 and 3) as were described for the monofunctional catalases. In large part this is because both types of enzyme are heme-containing, but it has the implication that the residues in the active site will have similar roles. The peroxidatic reaction presents another layer of complexity involving the use of organic electron donors for the reduction of compound I to the resting state via two one-electron transfers (reaction 4).

$$\text{Cpd I}(\text{Por}^{+\cdot}\text{-Fe}^{\text{IV}}\text{= O}) + 2\text{AH}_2 \rightarrow \text{Enz}(\text{Por-Fe}^{\text{III}}) + 2\text{AH}^{\bullet} + \text{H}_2\text{O} \quad (4)$$

In the presence of a suitable organic electron donor and low levels of $H_2O_2$, the peroxidatic reaction becomes significant. Unfortunately, the in vivo peroxidatic substrate for the catalase-peroxidases has not been identified, leaving the actual role of the peroxidatic reaction undefined.

## Phylogeny

The first review of KatG phylogeny appeared in 2000 and included 19 sequences [44]. The most recent report has included 58 sequences that have become available, the majority from bacteria but with five each from archaebacteria and fungi [12]. With the larger number of sequences in the data set, the tree is not as robust as the earlier tree, and several interpretations of structure are possible. When integrated into a conceptual tree of life, it is apparent that the catalase-peroxidases evolved much later than the heme-containing monofunctional catalases, and a significant frequency of lateral gene transfer is evident. Very significantly, the data are consistent with the interpretation that sometime after a lateral gene transfer event from bacteria to the eukaryotic ancestor, the plant peroxidases evolved from the catalase-peroxidases.

## Catalase-peroxidase structures

The first catalase-peroxidase HPI of *E. coli* was purified and characterized in 1979 [45], and the sequence of its encoding gene, *katG*, appeared in 1988 [46], providing the first catalase-peroxidase sequence and demonstrating the close phylogenetic link to plant peroxidases. It remained for the demonstration that KatG from *Mycobacterium tu-*

*berculosis* was responsible for the activation of the widely used antitubercular drug isoniazid (INH) [47] to bring the catalase-peroxidases into the spotlight. This led to extensive efforts around the world to crystallize the protein in order to characterize at the molecular level the interaction of the protein with the drug. Attempts to crystallize HPI from *E. coli* had commenced unsuccessfully in 1987, and success with the *M. tuberculosis* enzyme was no better. Persistence was finally rewarded in 2001 and 2002 with preliminary reports of the crystallization of catalase-peroxidases from the halophilic archaebacterium *Haloarcula marismortui* [48], from the cyanobacterium *Synechococcus* [49] and the Gram-negative bacterium *Burkholderia pseudomallei* [50], and of the C-terminal domain of HPI of *E. coli* [51]. The structure of the *H. marismortui* enzyme (HmCPx) at 2.0 Å was reported first [52], followed by the structure of the *B. pseudomallei* enzyme (BpKatG) at 1.7 Å [53]. There are obvious and clear similarities between the two enzymes, but the BpKatG structure presents a number of unusual features that provided potentially significant insights into the function of the enzyme. In addition, the structures have opened new avenues to studying the enzyme through the identification of specific structural features to be investigated. One view of the BpKatG dimer is presented in figure 2.

The asymmetric unit of both catalase-peroxidases contains two subunits related by noncrystallographic twofold symmetry, consistent with the predominant form of the enzyme in solution being a dimer. Each subunit is composed of 20-$\alpha$-helical sections joined by linker regions and just three or four $\beta$-strand segments, making the structure very different from monofunctional catalases. It had previously been proposed that the large gene size of *katG* had arisen through a gene duplication and fusion event [54], resulting in a gene with two distinct sequence-related domains. Further support for this hypothesis is evident in the conservation of ten pseudo-symmetry-related $\alpha$-helical segments in the N- and C-terminal domains for which the r.m.s. deviation of 133 C$\alpha$ carbons following superimposition is just 2.19 Å in BpKatG. Superimposition of the N-terminal domain of BpKatG onto the structures of cytochrome c peroxidase, ascorbate peroxidase and horseradish peroxidase revealed r.m.s. deviations for the same 133 C$\alpha$ atoms in the 10 $\alpha$-helical segments of 0.97 Å, 1.22 Å and 2.03 Å, respectively. Not surprisingly, the inactive C-terminal domain has suffered greater evolutionary drift, with the corresponding 113 C$\alpha$ atoms in 10 $\alpha$-helical segments having r.m.s. deviations of 3.62 Å, 3.75 Å and 4.06 Å, when compared with cytochrome c peroxidase, ascorbate peroxidase and horseradish peroxidase. The high similarity between the HMCPx and BpKatG is illustrated by the r.m.s. deviation of 0.43 Å for the 133 C$\alpha$ atoms and 1.05 Å for the 685 C$\alpha$ atoms.

The heme-containing active site is somewhat more deeply buried compared with peroxidases but is accessed through a similar funnel-shaped channel that approaches the heme laterally rather than perpendicularly as in monofunctional catalases (fig. 3). Interpretation of possible substrate binding sites is complicated by the presence of a deep crevasse on the side of the protein that could potentially be the binding site of a substrate and the existence of a second channel approaching a small central cavity near the heme that also contains a single metal ion in BpKatG. Not knowing the natural peroxidatic substrate makes assigning roles to these features speculative at this point. HmCpx differs considerably in having 28 sulfate, chloride or potassium ions in its structure, consistent with the halophilic origin of the organism and the high ionic strength required to stabilize the enzyme.

**Covalent linkage joining Trp-Tyr-Met**

The most striking and unusual feature in both catalase-peroxidase structures is a covalent structure involving the indole ring of the active site Trp (residue 111 in BpKatG) and the sulfur of a Met (264 in BpKatG) joined to the ortho positions of a Tyr ring (residue 238 in BpKatG) (fig. 4). The structure is clearly evident in the electron density maps, although the refined bond lengths are a bit longer than ideal for covalent bonds, and the bonds to the Tyr and Trp are not pure sp2 in character, deviating somewhat from planarity. Independent evidence for the existence of the covalent bonds has been obtained from a mass spectrometry analysis of tryptic digests of BpKatG [55]. Similar results pointing to the presence of the Trp-Tyr-Met adduct in HPI of *E. coli* were also obtained, confirming its presence in three catalase-peroxidases and supporting conjecture that the structure may be common to all catalase-peroxidases.

The obvious question posed by such a covalent structure is, what is its role? It had previously been shown that the active site Trp is essential for normal catalatic activity. Its replacement by Phe results in the loss of catalase activity and enhanced peroxidase activity in both HPI [56] and the *Synechocystis* KatG [57, 58]. Subsequent work has shown that replacement of either $Met_{264}$ [55] or $Tyr_{238}$ [59] has a similar effect in eliminating catalase activity with no effect or a positive effect on peroxidase activity. In other words, the complete adduct is required for catalatic activity but not for peroxidatic activity, providing a clear explanation for why the apparently closely related plant peroxidases have no, or only a vestige, of catalase activity. Given that the adduct is required for catalase activity, electronic or steric roles or a combination of both can be envisioned. A very precise and immovable positioning of the indole ring may be necessary for interaction with the reducing $H_2O_2$ in order that correct bond lengths leading to the transition state are realized. Alternatively or in addition, the adduct may alter the electronic environment on the indole, enhancing the interaction with the substrate

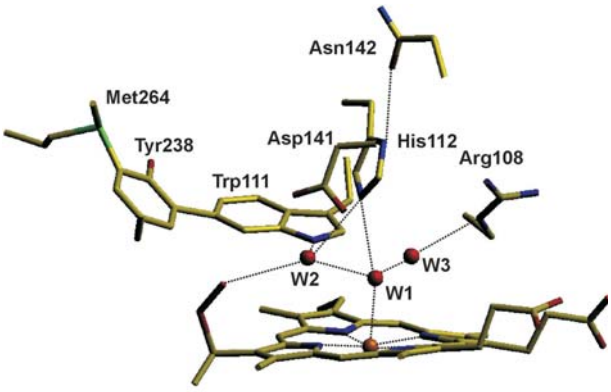


Figure 4. Structure of the distal side residues that are critical for catalatic activity in the catalase- peroxidases including the covalent adduct of $Trp_{111}$-$Tyr_{238}$-$Met_{264}$. The structure and residue numbering in BpKatG is shown. The structure is viewed looking into the active site from the access channel, resulting in the side chain of $Asp_{141}$ being located between the viewer and $Trp_{111}$. The heme group, including the hydroperoxy group on the vinyl group of ring I, is shown along with the three waters in the active site. Hydrogen-bonding interactions are indicated by dashed lines. Note that $Asp_{141}$ does not interact with any of the other residues in the diagram. The figure was prepared using SETOR [120].

and facilitating the formation of the transition state. Determination of the structures of the variants individually lacking each of the Trp, Tyr and Met residues involved in the adduct will provide valuable evidence about the role of the adduct.

A very intriguing question that has not been addressed so far is the reaction mechanism giving rise to the covalent structure. A variety of mechanisms might be proposed, but a free radical mechanism involving hydrogen peroxide as an oxidant for the formation of both covalent bonds is the simplest, and one version of such a mechanism is presented in figure 5. An oxidized heme intermediate may be involved in the formation of the nearby Trp-Tyr linkage but seems less likely in the case of the Tyr-Met linkage. The fact that the M264L variant loses significant activity could be interpreted as being a result of the absence of the Tyr-Trp portion because the Met-Tyr bond has to form first or because the Tyr-Trp adduct, if it is present, is not sufficient to promote the catalatic reaction. Determination of the structure of the M264L variant will provide insight into this question.

Given that peroxidases probably evolved from catalase-peroxidases [12], the loss of catalatic activity was as simple as disrupting the covalent adduct. Loss of the inactive C-terminal domain and shrinkage of the remaining protein through loss of looped regions also had to occur. This leads to the interesting question: was the progenitor of catalase-peroxidases a large subunit peroxidase that became catalase-proficient, or was it always a catalase that evolved peroxidatic activity? At the moment, there is no answer.

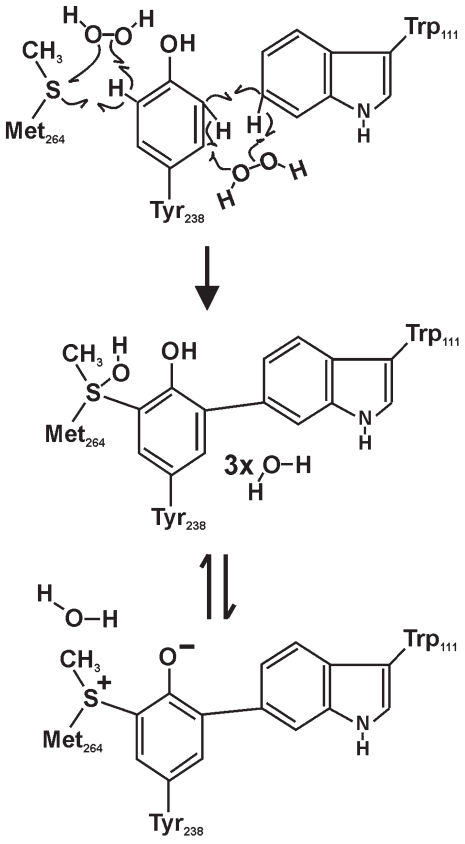


Figure 5. One possible mechanism for the creation of the covalent adduct among $Trp_{111}$, $Tyr_{238}$ and $Met_{264}$. Hydrogen peroxide catalyzes the covalent bond formation at both sites, and a free radical route is presented. The methionine S is left with a positive charge because the presence of oxygen is not indicated in the electron density maps, and this may be stabilized by the negative charge on the tyrosine, which can be associated with $Arg_{426}$.

## Heme modification

A second unusual modification in BpKatG [53], not evident in the HmCPx structure [52], is an apparent perhydroxy modification on the ring I vinyl group of the heme (fig. 4). The modification, first noticed in the electron density maps of BpKatG, has subsequently been confirmed by mass spectrometry analysis [55]. The modification could arise from the simple hydration-like addition of hydrogen peroxide across the double bond of the vinyl group. As such, its removal should be equally facile, and treatment of the enzyme with INH, a peroxidatic substrate, does cause its removal. Another indication of the labile nature of the modification is evident in the small amount of oxidized heme in the mass spectrum. The presence of an easily reversible modification involving the substrate in the active site presents a strong argument that it has some mechanistic significance. The simplest interpretation is that the perhydroxy group serves as a reservoir of $H_2O_2$. Normally, the heme would be oxidized to compound I by $H_2O_2$, but compound I is very reactive and

is rapidly degraded if substrate is not present. The perhydroxy modification is less reactive than compound I and allows $H_2O_2$ to reside in the active site, available for immediate reaction when a peroxidatic substrate is contacted.

**INH activation**

How does KatG activate INH to be an antitubercular substance? The initial KatG-catalyzed removal of the hydrazine portion of INH, generating the isonicotinoyl radical, presumably involves oxidation of the hydrazide radical to diimide and reduction of compound I or II. The subsequent step of combining the acyl radical with $NAD^+$ to generate the adduct that binds to InhA to inhibit mycolic acid synthesis is not as clearly defined. Initially, the adduct was characterized in the active site of InhA, leading to the conclusion that it was formed in InhA [60], although this would have necessitated the transfer of a radical species from KatG to InhA. Subsequently, it was suggested that the isonicotinoyl radical and $NAD^+$ reacted independent of protein via the Minisci reaction [61]. The requirement of KatG for rapid radical generation and InhA-inhibitor generation leads to the conclusion that KatG was responsible for both [62]. Unfortunately, with KatG in the reaction mixture, it is not possible to define clearly the extent of its involvement. Is the role of KatG limited to radical production, or does it also facilitate the addition of the radical to $NAD^+$? At the moment, we can only state that KatG greatly enhances the production of the isonicotinoyl-$NAD^+$ inhibitor of InhA through the generation of isonicotinoyl radical, but the involvement of KatG or any other protein in the addition of the acyl radical to $NAD^+$ has not been convincingly demonstrated.

The structure of BpKatG contains a region of unassigned electron density of a size and shape consistent with a molecule similar to INH and in a location consistent with being the INH binding site (fig. 3). Because the enzyme used for crystallization had never been treated with INH and INH is not a natural metabolite, the unknown ligand in BpKatG must be a metabolite with a structure similar to INH. A number of pyridine-based coenzymes, such as pyridoxal phosphate and nicotinamide, come immediately to mind. The structure surrounding the ligand can easily be rationalized as a site for radical generation and electron transfer to the heme in MtKatG involving, in particular, $Ser_{324}$ (fig. 3), the equivalent of $Ser_{315}$ the most prevalent site for mutations causing INH resistance [63]. The unknown ligand is near the narrow end of the funnel-shaped entrance channel, and $NAD^+$ could potentially fit into the funnel, placing it in close proximity to the nascent radical. Hence, it is physically possible for KatG to be involved in the generation of the InhA inhibitor, but $NAD^+$ binding to KatG has never been demonstrated.

**KatG variant characterization**

Biochemical analyses of the catalase-peroxidases have been proceeding in parallel with the structural work. The *Synechocystis*, *E. coli* and *M. tuberculosis* catalase-peroxidases have been extensively dissected through a combination of site-directed mutagenesis and characterization of the variants. The *M. tuberculosis katG* has been modified to express a number of naturally occurring KatG variants that impart INH resistance [64, 65]. A comparison of the variant properties with the location of the residue change in the protein structure reveals three categories of mutations [53]. The first category, and possibly the most interesting, includes only the S315T variant, which interferes with INH activation without significantly reducing peroxidatic activity. As noted above, an INH-like molecule is bound adjacent to and appears to interact with the main-chain atoms in the residue equivalent to $Ser_{324}$ in BpKatG, suggesting a mechanism for how the MtKatG S315T change might affect INH binding. With no change in main-chain conformation, the Thr side chain would interact with the heme propionate, forcing a rotation of the Thr side chain. This would break the propionate-OH link, a likely electron transfer conduit between the heme and the active site. In order to maintain the propionate-SerOH association, a distortion of the main-chain atoms is required, and this would sterically interfere with INH binding. Electronic absorption and resonance Raman spectroscopy suggest that while there are differences in the heme between the native and S315T variant, the variant actually stabilizes the native conformation in the long term [66]. Recent calorimetric and spectroscopic characterization has concluded that the change from Ser to Thr reduces the affinity of the enzyme for INH [67], consistent with the concept that disturbance of the main chain around $Thr_{315}$ is the explanation for poor INH binding.

The second group of MtKatG mutations includes a larger number of variants that interfere generally with peroxidatic activity by disrupting the matrix of active-site residues in the vicinity of the heme. The third category includes a number of residues that are quite distant from the active site, some resident in the C-terminal domain, suggesting that they interfere either with protein folding or with subunit association. This interpretation is supported by the lack of protein accumulation on expression.

The initial mutageneses of *E. coli* HPI and *Synechocystis* KatG (SyKatG) were focused on the active-site residues and generally confirmed the importance of the distal side triad of Arg (102 in HPI, 119 in SyKatG), Trp (105 in HPI, 122 in SyKatG) and His (106 in HPI, 123 in SyKatG), and $His_{267}$ as the proximal side ligand of the heme iron in HPI [56–58]. Perhaps the most exciting observation was that changing $Trp_{105}$ (HPI) or $Trp_{122}$ (SyKatG) for Phe, a common change in plant peroxidases, resulted in loss of catalase activity and an increase

in peroxidatic activity. The ready accumulation of a compound I radical was demonstrated, confirming the importance of the distal Trp in the second stage of the catalatic reaction and its lack of importance in the first-stage formation of compound I. More recently, the distal side $Asp_{152}$ [68] and $Asn_{153}$ [69] of SyKatG were also found to be critical for catalatic activity, but not for peroxidatic activity. These two residues are conserved in all known catalase-peroxidase sequences except that of *Salmonella typhimurium* [70], where the Asn is replaced by a Thr. Given the similar codon sequences, ACPy for Thr and AAPy, this one exception may eventually prove to be the result of a sequencing error. A continuation of this common theme of an independent loss of catalatic activity also occurs in the replacement of either $Tyr_{249}$ of SyKatG [59] or $Met_{268}$ of BpKatG [55]. Both these residues are involved in the covalent adduct, and in their absence there is a significant reduction in catalase activity with little effect on peroxidase activity. These catalase-defective variants have provided a perfect opportunity to study the peroxidatic activity of the enzyme in comparison with plant peroxidases, revealing that the mechanisms of compound I formation and overall peroxidatic rates are similar between the two classes of enzyme. Whether the compound I radical proves to be a uniquely porphyrin cation radical [59] or a tyrosine radical [71] in all catalase-peroxidases or whether different enzymes will have different radical locations will be the subject of further study.

At this time, the catalogue of residues required for catalatic activity in the catalase-peroxidases includes the $Trp_{111}$, $Asp_{141}$, $Asn_{142}$, $Tyr_{238}$ and $Met_{264}$ (BpKatG numbering and residues 122, 152, 153, 249 and 275, respectively, in SyKatG). Each of these changes is essential, and it will be interesting to see how many more residues will be found to be essential for catalatic activity. One feature unique to the catalase-peroxidases is the large subunit-2 domain structure, and it is not yet clear whether both domains are required for catalatic activity.

## Nonheme or manganese-containing catalases

Nonheme catalases were initially referred to as pseudocatalases because they did not contain heme [72], but other names, including Mn-containing [73], nonheme [2] and dimanganese catalase [74] more accurately reflect their characteristics and have been applied. The nonheme catalases are not as widespread as the heme-containing catalases and so far have been identified only in bacteria. The number of available sequences has recently increased to 29, allowing for a phylogenetic review, and the resulting tree presents two main groups and suggests that the class of enzymes appeared at a time intermediate between the early appearance of monofunctional catalases and the late appearance of catalase-peroxidases [12]. It is speculated that the dimanganese catalases may not have become as widespread in nature because of their lower specific activity in relation to other catalases that already existed in multiple forms in many bacteria.

The crystal structures of the two nonheme catalases, one from *Thermus thermophilus* (TTC) [74] and the second from *Lactobacillus plantarum* (LPC) [75] reveal that the catalytic center is a dimanganese group. The enzyme is a homohexameric structure of approximately 30 kDa monomers (fig. 2). The four-helix bundle motif of the individual monomers is highly conserved between the two enzymes, with only the C-terminal tails differing. The dimanganese centers share very similar environments, with the direct coordination of the Mn atoms involving a virtually identical matrix of glutamate and histidine residues. The environments differ slightly in that one glutamate that normally interacts with Mn-associated waters in LPC is replaced by an arginine in TTC, and an arginine in LPC is absent in TTC. Access to the dimanganese clusters is via a central channel that extends the full width of the hexamer, with branches into each subunit leading to the active center. The branch leading from the central channel into one of the dimanganese clusters is shown in figure 3, and the similarity in length and narrowness of the channel to those in the monofunctional catalases is quite striking. In all three cases, CatF, HPII and LPC, the final 15 Å is uniformly narrow as compared with the funnel shape of the channel in the catalase-peroxidases, suggesting that restricted access to only substrate $H_2O_2$ is very important to the catalatic reaction. The absence of a glutamate and an arginine in the TTC active site apparently creates a larger cavity and a second access channel that allows in larger ions that cannot reach the LPC active site, but viewing this expanded channel will have to await the release of the TTC coordinates.

The dimanganese catalase structures provide insight into the mechanism of the catalatic reaction in a nonheme environment. Like heme-containing catalases, the reaction takes place in two stages, but here the similarity ends. The oxidation state of the dimanganese cluster is equally stable in either the 2,2 ($Mn^{II}$-$Mn^{II}$) or 3,3 ($Mn^{III}$-$Mn^{III}$) states, resulting in the enzyme being isolated primarily as a mixture of these two states. Consequently, there is no temporal order to the oxidation and reduction stages, and either can occur first depending on the resting state of the enzyme. If the 2,2 state is encountered, the $H_2O_2$ is an oxidant (reaction 5) and if the 3,3 state is encountered, the $H_2O_2$ is a reductant (reaction 6).

$$H_2O_2 + Mn^{II}\text{-}Mn^{II}(2H^+) \rightarrow Mn^{III}\text{-}Mn^{III} + 2\,H_2O \quad (5)$$

$$H_2O_2 + Mn^{III}\text{-}Mn^{III} \rightarrow Mn^{II}\text{-}Mn^{II}(2H^+) + O_2 \quad (6)$$

Reactions 5 and 6 are presented as being analogous to reactions 2 and 3 in heme-containing catalases, but there is one overriding difference. Oxidation of the reaction center (reaction 5) involves removal of electrons from the ac-

tive center, but a derivatized reactive intermediate is not produced. As a result, the second stage does not involve reduction of a reactive intermediate, but a simple transfer of electrons to the dimanganese center generating oxygen. Another nuance is that both product waters are generated in reaction 5, unlike the heme catalases, where one water is produced in each of reactions 2 and 3.

*Acknowledgement.* Preparation of this manuscript was supported by Grant OGP9600 from the Natural Sciences and Engineering Research Council of Canada to P. C. Loewen.


1 Loew O. (1900) Physiological studies of Connecticut leaf tobacco. U.S. Dept. of Agri. Repts. **56:** 5–57
2 Nicholls P., Fita I. and Loewen P. C. (2001) Enzymology and structure of catalases. Adv. Inorg. Chem. **51:** 51–106
3 Maté M. J., Murshudov G., Bravo J., Melik-Adamyan W., Loewen P. C. and Fita I. (2001) Heme catalases. In: Handbook of Metalloproteins, pp. 486–502, Messerschmidt A., Huber R., Poulos T. and Widghardt K. (eds), Wiley & Sons, Chichester, U.K.
4 Klotz M. G., Klassen G. R. and Loewen P. C. (1997) Phylogenetic relationships among prokaryotic and eukaryotic catalases. Mol. Biol. Evol. **14:** 951–958
5 Loewen P. C. (1997) Bacterial catalases. In: Oxidative Stress and the Molecular Biology of Antioxidant Defenses, pp. 273–308. Scandalios J. G. (ed), Cold Spring Harbor
6 Jung I. L. and Kim I. G. (2003) Transcription of *ahpC*, *katG* and *katE* genes in *Escherichia coli* is regulated by polyamines: polyamine-deficient mutant sensitive to $H_2O_2$-induced oxidative damage. Biochem. Biophys. Res. Commun. **301:** 915–922
7 Horsburgh M. J., Clements M. O., Crossley H., Ingham E. and Foster S. J. (2001) PerR controls oxidative stress resistance and iron storage proteins and is required for virulence in *Staphylococcus aureus*. Infect. Immun. **69:** 3744–5374
8 Ma J. F., Ochsner U. A., Klotz M. G., Nanayakkara V. K., Howell M. L., Johnson Z. et.al. (1999) Bacterioferritin A modulates catalase A (KatA) activity and resistance to hydrogen peroxide in *Pseudomonas aeruginosa*. J. Bacteriol. **181:** 3730– 3742
9 Helmann J. D., Wu M. F., Gaballa A., Kobel P. A., Morshedi M. M., Fawcett P. et al. (2003) The global transcriptional response of *Bacillus subtilis* to peroxide stress is coordinated by three transcription factors. J. Bacteriol. **185:** 243–253
10 Andreoletti P., Sainz G., Jaquinod M., Gagnon J. and Jouve, H. M. (2003) High resolution structure and biochemical properties of a recombinant *Proteus mirabilis* catalase depleted in iron. Proteins **50:** 261–271
11 Von Ossowski I., Hausner G. and Loewen P. C. (1993) Molecular evolutionary analysis based on the amino acid sequence of catalase. J. Mol. Evol. **37:** 71–76
12 Klotz M. G. and Loewen P. C. (2003) The molecular evolution of catlatic hydroperoxidases: evidence for multiple lateral transfer of genes between prokaryota and from bacteria into eukaryota. Mol. Biol. Evol. **20:** 1098–1112
13 Switala J. and Loewen P. C. (2002) Diversity of properties among catalases. Arch. Biochem. Biophys. **401:** 145–154
14 Meir E. and Yagil E. (1984) Catalase-negative mutants of *Escherichia coli*. Curr. Microbiol. **11:** 13–18
15 Goldberg I. and Hochman A. (1989) Three different types of catalases in *Klebsiella pneumoniae*. Arch. Biochem. Biophys. **268:** 124–128
16 Switala J., O'Neil J. O. and Loewen P. C. (1999) Catalase HPII from *Escherichia coli* exhibits enhanced resistance to denaturation. Biochemistry **38:** 3895–3901
17 Chelikani P., Donald L. J., Duckworth H. W. and Loewen P. C. (2003) Hydroperoxidase II of *Escheriochia coli* exhibits enhanced resistance to proteolytic cleavage compared to other catalases. Biochemistry **42:** 5729–5735
18 Sevinc M. S., Switala J., Bravo J., Fita I. and Loewen P. C. (1998) Truncation and heme pocket mutations reduce production of functional catalase HPII in *Escherichia coli*. Protein Eng. **11:** 549–555
19 Ueda M., Kinoshita H., Maeda S. I., Zou W. and Tanaka A. (2003) Structure-function study of the amino-terminal stretch of the catalase subunit molecule in oligomerization, heme binding and activity expression. Appl. Microbiol. Biotechnol. **61:** 488–494
20 Murthy M. R. N., Reid T. J., Sicignano A., Tanaka N. and Rossmann M.G. (1981) Structure of beef liver catalase. J. Mol. Biol. **152:** 465–499
21 Fita I., Silva A. M., Murthy M. R. N. and Rossmann M. G. (1986) The refined structure of beef liver catalase at 2.5 A resolution Acta Crystallogr. B**42:** 497–515
22 Murshudov G. N., Melik-Adamyan W. R., Grebenko A. I., Barynin V. V., Vagin A. A., Vainshtein B. K. et al. (1982) Three-dimensional structure of catalase from *Micrococcus lysodeikticus* at 1.5Å resolution. FEBS Lett. **312:** 127–131
23 Gouet P., Jouve H. M. and Dideberg O. (1995) Crystal structure of *Proteus mirabilis* PR catalase with and without bound NADPH. J. Mol. Biol. **249:** 933–954
24 Berthet S., Nykyri L., Bravo J., Maté M. J., Berthet-Colominas C., Alzari P. M. et al. (1997) Crystallization and preliminary structural analysis of catalase-A from *Saccharomyces cerevisiae*. Protein Sci. **6:** 481–483
25 Maté M. J., Zamocky M., Nykyri L. M., Herzog C., Alzari P. M., Betzel C. et al. (1999) Structure of catalase-A from *Saccharomyces cerevisiae*. J. Mol. Biol. **286:** 135–139
26 Putnam C. D., Arvai A. S., Bourne Y. and Tainer J.A. (1999) Active and inhibited human catalase sturctures: ligand and NADPH binding and catalytic mechanism. J. Mol. Biol. **296:** 295–309
27 Vainshtein B. K., Melik-Adamyan W. R., Barynin V. V., Vagin A. A. and Grebenko A. I. (1981) Three-dimensional structure of the enzyme catalase. Nature **293:** 411–412
28 Vainshtein B. K., Melik-Adamyan W. R., Barynin V. V., Vagin A. A., Grebenko A. I., Borisov V. V. et al. (1986) Three-dimensional structure of catalase from *Penicillium vitale*, at 2.0 Å resolution. J. Mol. Biol. **188:** 49–61
29 Bravo J., Verdaguer N., Tormo J., Betzel C., Switala J., Loewen P. C. et al. (1995) Crystal structure of catalase HPII from *Escherichia coli*. Structure **3:** 491–502
30 Bravo J., Maté M. J., Schneider T., Switala J., Wilson K., Loewen P. C. et al. (1999) Structure of catalase HPII from *Escherichia coli* at 1.9 Å resolution. Proteins **34:** 155–166
31 Carpena X., Perez R., Ochoa W. F., Verdaguer N., Klotz M. G., Switala J. et al. (2001) Crystallization and preliminary X-ray analysis of clade I catalases from *Pseudomonas syringae* and *Listeria seeligeri*. Acta Crystallograph. D**57:** 1184–1186
32 Carpena X., Soriano M., Klotz M. G., Duckworth H. W., Donald L. J., Melik-Adamyan W. et al. (2003) Structure of the clade 1 catalase, CatF of *Pseudomonas syringae*, at 1.8 Å resolution. Proteins **50:** 423–436
33 Murshudov G. N., Grebenko A. I., Barynin V., Dauter Z., Wilson K. S., Vainshtein B. K. et al. (1996) Structure of heme d of *Penicillium citale* and *Escherichia coli*. J. Biol. Chem. **271:** 8863–8868
34 Kirkman H. N. and Gaetani G. F. (1984) Catalase: a tetrameric enzyme with four tightly bound molecules of NADPH. Proc. Natl. Acad. Sci. USA **81:** 4343–4347
35 Hillar A. and Nicholls P. (1992) A mechanism for NADPH inhibition of catalase compound II formation. FEBS Lett. **314:** 179–182

36 Olson L. P. and Bruice T. C. (1995) Electron tunneling and ab initio calculations related to the one-electron oxidation of NAD(P)H bound to catalase. Biochemistry **34:** 7335–7347
37 Almarsson O., Sinha A., Gopinath E. and Bruice T. C. (1993) Mechanism of one-electron oxidation of NAD(P)H and function of NADPH bound to catalase. J. Am. Chem. Soc. **115:** 7093–7102
38 Kirkman H. N., Rolfo M., Ferraris A, M. and Gaetani G. F. (1999) Mechanisms of protection of catalase by NADPH. Kinetics and stoichiometry. J. Biol. Chem. **274:** 13908–13914
39 Heck D. E., Vetrano A. M., Marian T. M. and Laskin J. D. (2003) UVB light stimulates production of reactive oxygen species: unexpected role for catalase. J. Biol. Chem., in press
40 Chelikani P., Carpena X., Fita I, and Loewen P. C. (2003) An electrical potential in the access channel of catalases enhances catalysis. J. Biol. Chem. **278:** 31290–31296
41 Kalko S. G., Gelpi J. L., Fita I. and Orozco M. (2001) Theoretical study of the mechanisms of substrate recognition by catalase. J. Am. Chem. Soc. **123:** 9665–9672
42 Amara P., Andreoletti P., Jouve H. M. and Field M. J. (2001) Ligand diffusion in the catalase from *Proteus mirabilis*: a molecular dynamics study. Protein Sci. **10:** 1927–1935
43 Loewen P. C., Switala J., von Ossowski I., Hillar A., Christie A., Tattrie B. and Nicholls P. (1993) Catalase HPII of *Escherichia coli* catalyzes the conversion of protoheme to *cis*-heme d. Biochemistry **32:** 10159–10164
44 Faguy D. M. and Doolittle W. F. (2000) Horizontal transfer of catalase-peroxidase genes between Archaea and pathogenic bacteria. Trends Genet. **16:** 196–197
45 Claiborne A. and Fridovich I. (1979) Purification of the o-dianisidine peroxidase from *Escherichia coli* B. J. Biol. Chem. **254:** 4245–4252
46 Triggs-Raine B. L., Doble B. W., Mulvery M. R., Sorby P. A. and Loewen P. C. (1988) Nucleotide sequence of *katG*, encoding catalase HPI of *Escherichia coli*. J. Bacteriol. **170:** 4415–4419
47 Zhang Y., Heym B., Allen B., Young D. and Cole S. (1992) The catalase-peroxidase gene and isoniazid resistance of *Mycobacterium tuberculosis*. Nature **358:** 591–593
48 Yamada Y., Saijo S., Sato T., Igarashi N., Usui H., Fujiwara T. et al. (2001) Crystallization and preliminary X-ray analysis of catalase-peroxidase from the halophilic archaeon *Haloarcula marismortui*. Acta Cryst. D**57:** 1157–1158
49 Wada K., Tada T., Nakamura Y., Kinoshita T., Tamoi M., Sigeoka S. et al. (2002) Crystallization and preliminary X-ray diffraction studies of catalase-peroxidase from Synechococcus PCC7492. Acta Cryst. D**58:** 157–159
50 Carpena X., Switala J., Loprasert S., Mongkolsuk S., Fita I. and Loewen, P. C. (2002) Crystallization and preliminary X-ray analysis of the catalase-peroxidase KatG from *Burkholderia pseudomallei*. Acta Cryst. D**58:** 2184–2186
51 Carpena X., Guarne A., Ferrer J. C., Alzari P. M., Fita I. and Loewen, P. C. (2002) Crystallization and preliminary X-ray analysis of the hydroperoxidase I C-terminal domain from *Escherichia coli*. Acta Cryst. D**58:** 853–855
52 Yamada Y., Fujiwara T., Sato T., Igarashi N. and Tanaka N. (2002) The 2.0 Å crystal structure of catalase-peroxidase from *Haloarcula marismortui*. Nat. Struct. Biol. **9:** 691–695
53 Carpena X., Loprasert S., Mongkolsuk S., Switala J., Loewen P. C. and Fita I. (2003) Catalase-peroxidase KatG of Burkholderia pseudomallei at 1.7 Å resolution. J. Mol. Biol. **327:** 475–489
54 Welinder, K. G. (1991) Bacterial catalase-peroxidases are gene duplicated members of the plant peroxidase superfamily. Biochim. Biophys. Acta **1080:** 215–220
55 Donald L. J., Krokhin O. V., Duckworth H. W., Wiseman B., Deemagarn T., Singh R. et al. (2003) Characterization of the catalase-peroxidase KatG from *Burkholderia pseudomallei* by mass spectrometry. J. Biol. Chem., in press
56 Hillar A., Peters B., Pauls R., Loboda A., Zhang H., Mauk A. G. et al. (2000) Modulation of the activities of catalase-peroxidase HPI of *Escherichia coli* by site directed mutagenesis. Biochemistry **39:** 5868–5875
57 Regelsberger G., Jakopitsch C., Ruker F., Krois D., Peschek G. A. and Obinger C. (2000) Effect of distal cavity mutations on the formation of compound I in catalase-peroxidases. J. Biol. Chem. **275:** 22854–22861
58 Regelsberger G., Jakopitsch C., Furtmuller P. G., Rueker F., Switala J., Loewen P. C. et al. (2001) The role of distal tryptophan in the bifunctional activity of catlase-peroxidases. Biochem. Soc. Trans. **29:** 99–105
59 Jakopitsch C., Auer M., Ivancich A., Rüker F., Furtmüller P. G. and Obinger C. (2003) Total conversion of bifunctional catalase-peroxidase (KatG) to monofunctional peroxidase by exchange of a conserved distal side tyrosine. J. Biol. Chem. **278:** 20185–10191
60 Rozawarski D. A., Grant G. A., Barton D. H. R., Jacobs Jr W. R. and Sacchettini J. C. (1998) Modification of the NADH of the isoniazid target (INHA) from *Mycobacterium tuberculosis*. Science **279:** 98–102
61 Wilming M. and Johnsson K. (1999) Spontaneous formation of the bioactive form of the tuberculosis drug isoniazid. Angew. Chem. Int. Ed. **38:** 2588–2590
62 Lei B., Wei C. J. and Tu S. C. (2000) Activation mechanism of antitubercular isoniazid: activation by *Mycobacterium tuberculosis* KatG, isolation and characterization of InhA inhibitor. J. Biol. Chem. **275:** 2520–2526
63 Ramaswamy S. and Musser J. M. (1998) Molecular genetic basis of antimicrobial agent resistance in *Mycobacterium tuberculosis*: 1998 update. Tuberc. Lung Dis. **79:** 3–29
64 Saint-Joanis B., Souchon H., Wilming M., Johnsson K., Alzari P. and Cole S. T. (1999) Use of site-directed mutagenesis to probe the structure, function and isonizid activation of the catlase/peroxidase, KatG, from *Mycobacterium tuberculosis*. Biochem. J. **338:** 753–760
65 Rouse D. A., DeVito J. A., Li Z., Byer H. and Morris S. L. (1996) Site-directed mutagenesis of the *katG* gene of *Mycobacterium tuberculosis*: effects on catalase-peroxidase activities and isoniazid resistance. Mol. Microbiol. **22:** 583–592
66 Kapetanaki S., Couchane S., Girotto S., Yu S., Magliozzo R. S. and Schelvis J. P. M. (2003) Conformational differences in *Mycobacterium tuberculosis* catalase-peroxidase KatG and its S315T mutant revealed by resonance Raman spectroscopy. Biochemistry **42:** 3835–3845.
67 Yu S., Girotto S., Lee C. and Magliozzo R. S. (2003) Reduced affinity for isoniazid in the S315T mutant of *Mycobacterium tuberculosis* KatG is a key factor in antibiotic resistance. J. Biol. Chem. **278:** 14769–14775
68 Jakopitsch C., Auer M., Regelsberger, G., Jantschko W., Furtmüller P. G., Rüker F. et al. (2003) Distal site aspartate is essential in the catalase activity of catalase-peroxidases. Biochemistry **42:** 5292–5300
69 Jakopitsch C., Auer M., Regelsberger, G., Jantschko W., Furtmüller P. G., Rüker F. et al. (2003) The catalytic role of the distal site asparagine-histidine couple in catalase-peroxidases. Eur. J. Biochem. **270:** 1006–1013
70 Loewen P. C. and Stauffer G. V. (1990) Nucleotide sequence of *katG* of *Salmonella typhimurium* and characterization of its product, hydroperoxidase I. Mol. Gen. Genet. **224:** 147–151
71 Couchane S., Girotto S., Yu S. and Magliozzo R. S. (2002) Identification and characterization of tyrosyl radical formation in *Mycobacterium tuberculosis* catalase-peroxidase (KatG). J. Biol. Chem. **277:** 42633–42638
72 Kono Y. and Fridovich I. (1983) Isolation and characterization of the pseudocatalase of *Lactobacillus plantarum*. A new manganese containing enzyme. J. Biol. Chem. **258:** 6015–6019

73 Allgood G. S. and Perry J. J. (1986) Characterization of a manganese-containing catalase from the obligate thermophile *Thermoleophilum album*. J. Bacteriol. **168:** 563–567

74 Antonyuk S. V., Melik-Adamyan V. R., Popov A. N., Lamzin V. S., Hampstead P. D., Harrison P. M. et al. (2000) Three-dimensional structure of the enzyme dimanganese catalase from *Thermus Thermophilus* at 1 Å resolution. Crystallogr. Reports **45:** 105–116

75 Barynin V. V., Whittaker M. M., Antonyuk S. V., Lamzin V. S., Harrison P. M., Artymiuk P. J. et al. (2001) Crystal structure of manganese catalase from *Lactobacillus plantarum*. Structure **9:** 725–738

76 Nakjarung K., Mongkolsuk S. and Vattanaviboon P. (2003) The oxyR from *Agrobacterium tumefaciens*: evaluation of its role in the regulation of catalase and peroxide responses. Biochem. Biophys. Res. Commun. **304:** 41–47

77 Navarro R. E. and Aguirre J**.** (1998) Posttranscriptional control mediates cell type-specific localization of catalase A during *Aspergillus nidulans* development. J. Bacteriol. **180:** 5733–5738

78 Kawasaki L., Wysong D., Diamond R. and Aguirre J. (1997) Two divergent catalase genes are differentially regulated during *Aspergillus nidulans* development and oxidative stress. J. Bacteriol. **179:** 3284–3292

79 Kawasaki L. and Aguirre J. (2001) Multiple catalase genes are differentially regulated *Aspergillus nidulans*. J. Bacteriol. **183:** 1434–1440

80 Scherer M., Wei H., Liese R. and Fischer R. (2002) *Aspergillus nidulans* catalase-peroxidase gene (cpeA) is transcriptionally induced during sexual development through the transcription factor StuA. Eukaryot. Cell **1:** 725–735

81 Witteveen F. B., van de Vondervoort P. J., van den Broeck H. C., van Engelenburg A. C., de Graaff L. H., Hillebrand M. H., et al. (1993) Induction of glucose oxidase, catalase and lactonase in *Aspergillus niger*. Curr. Genet. **24:** 408–416

82 Hicks D. B. (1995) Purification of three catalase isozymes from facultatively alkaliphilic *Bacillus firmus* OF4. Biochim. Biophys. Acta **1229:** 347–355

83 Bsat N., Herbig A., Casillas-Martinez L., Setlow P. and Helmann J. D. (1998) *Bacillus subtilis* contains multiple Fur homologues: identification of the iron uptake (Fur) and peroxide regulon (PerR) repressors. Mol. Microbiol. **29:** 189–198

84 Bol D. K. and Yasbin R. E. (1994) Analysis of the dual regulatory mechanisms controlling expression of the vegetative catalase gene of *Bacillus subtilis*. J. Bacteriol. **176:** 6744– 6748

85 Engelmann S., Lindner C. and Hecker M. (1995) Cloning, nucleotide sequence and regulation of katE encoding a sigma B-dependent catalase in *Bacillus subtilis* J. Bacteriol. **177:** 5598–5605

86 Bagyan I., Casillas-Martinez L. and Setlow P. (1998) The katX gene, which codes for the catalase in spores of *Bacillus subtilis*, is a forespore-specific gene controlled by sigmaF, and KatX is essential for hydrogen peroxide resistance of the germinating spore. J. Bacteriol. **180:** 2057–2062

87 Rocha E. R., Owens G. Jr and Smith C. J. (2000) The redox-sensitive transcriptional activator OxyR regulates the peroxide response regulon in the obligate anaerobe *Bacteroides fragilis*. J. Bacteriol. **182:** 5059–5069

88 Kim J. A. and Mayfield J. (2000) Identification of *Brucella abortus* OxyR and its role in control of catalase expression. J. Bacteriol. **182:** 5631–5633

89 Wang P. and Schellhorn H. E. (1995) Induction of resistance to hydrogen peroxide and radiation in *Deinococcus radiodurans*. Can. J. Microbiol. **41:** 170–176

90 Christman M. F., Storz G. and Ames B. N. (1989) OxyR, a positive regulator of hydrogen peroxide-inducible genes in *Escherichia coli* and *Salmonella typhimurium*, is homologous to a family of bacterial regulatory proteins. Proc. Natl. Acad. Sci. USA **86:** 3484–3488

91 Loewen P. C., Switala J. and Triggs-Raine B. L. (1985) Catalases HPI and HPII in *Escherichia coli* are induced independently. Arch. Biochem. Biophys. **243:** 144–149

92 Bishai W. R., Smith H. O. and Barcak G. J. (1994) A peroxide/ascorbate-inducible catalase from *Haemophilus influenzae* is homologous to the *Escherichia coli* katE gene product. J. Bacteriol. **176:** 2914–2921

93 Odenbreit S., Wieland B. and Haas R. (1996) Cloning and genetic characterization of *Helicobacter pylori* catalase and construction of a catalase-deficient mutant strain. J. Bacteriol. **178:** 6960–6967

94 Harris A. G, Hinds F. E., Beckhouse A. G., Kolesnikow T. and Hazell S. L. (2002) Resistance to hydrogen peroxide in *Helicobacter pylori*: role of catalase (KatA) and Fur, and functional analysis of a novel gene product designated 'KatA-associated protein', KapA (HP0874). Microbiology **148:** 3813–3825

95 Zahrt T. C., Song J., Siple J. and Deretic V. (2001) Mycobacterial FurA is a negative regulator of catalase-peroxidase gene katG. Mol. Microbiol. **39:** 1174–1185

96 Pym A. S., Domenech P., Honore N., Song J., Deretic V. and Cole S. T. (2001) Regulation of catalase-peroxidase (KatG) expression, isoniazid sensitivity and virulence by furA of *Mycobacterium tuberculosis*. Mol. Microbiol. **40:** 879–889

97 Tseng H. J., McEwan A. G., Apicella M. A. and Jennings M. P. (2003) OxyR acts as a repressor of catalase expression in *Neisseria gonorrhoeae*. Infect. Immun. **71:** 550–556

98 Calcutt M. J., Becker-Hapak M., Gaut M., Hoerter J. and Eisenstark A. (1998) The rpoS gene of *Erwinia carotovora*: gene organization and functional expression in *E. coli*. FEMS Microbiol. Lett. **159:** 275–281

99 Hassett D. J., Sokol P. A., Howell M. L., Ma J. F., Schweizer H. T., Ochsner U. et al. (1996) Ferric uptake regulator (Fur) mutants of *Pseudomonas aeruginosa* demonstrate defective siderophore-mediated iron uptake, altered aerobic growth and decreased superoxide dismutase and catalase activities. J. Bacteriol. **178:** 3996–4003

100 Ochsner U.A., Vasil M.L., Alsabbagh E., Parvatiyar K. and Hassett D.J. (2000) Role of the *Pseudomonas aeruginosa* oxyR-recG operon in oxidative stress defense and DNA repair: OxyR-dependent regulation of katB-ankB, ahpB and ahpC-ahpF. J. Bacteriol. 182**:** 4533–4544

101 Katsuwon J. and Anderson A. J. (1989) Response of plant-colonizing pseudomonads to hydrogen peroxide. Appl. Environ. Microbiol. **55:** 986–989

102 Klotz M. G. and Hutcheson S. W. (1992) Multiple periplasmic catalases in phytopathogenic strains of *Pseudomonas syringae*. Appl. Environ. Microbiol. **58:** 2468–2473

103 Amo T., Atomi H. and Imanaka T. (2002) Unique presence of a manganese catalase in a hyperthermophilic archaeon, *Pyrobaculum calidifontis* VA1. J. Bacteriol. **184:** 3305–3312

104 Del Carmen Vargas M., Encarnacion S., Davalos A., Reyes-Perez A., Mora Y., Garcia-De Los Santos A. et al. (2003) Only one catalase, katG, is detectable in *Rhizobium etli* and is encoded along with the regulator OxyR on a plasmid replicon. Microbiology **149:** 1165–1176

105 Robbe-Saule V., Coynault C., Ibanez-Ruiz M., Hermant D. and Norel F. (2001) Identification of a non-haem catalase in *Salmonella* and its regulation by RpoS (sigmaS). Mol. Microbiol. **39:** 1533–1545

106 Christman M. F., Morgan R. W., Jacobson F. S. and Ames B. N. (1985) Positive control of a regulon for defenses against oxidative stress and some heat-shock proteins in *Salmonella typhimurium*. Cell **41:** 753–762

107 Fang F. C., Libby S. J., Buchmeier N. A., Loewen P. C., Switala J., Harwood J. et al. (1992) The alternative sigma factor katF (rpoS) regulates *Salmonella virulence*. Proc. Natl. Acad. Sci. USA **89:** 11978–11982

108 Ohwada T., Shirakawa Y., Kusumoto M., Masuda H. and Sato T. (1999) Susceptibility to hydrogen peroxide and catalase activity of root nodule bacteria. Biosci. Biotechnol. Biochem. **63:** 457–462
109 Herouart D., Sigaud S., Moreau S., Frendo P., Touati D. and Puppo A. (1996) Cloning and characterization of the katA gene of *Rhizobium meliloti* encoding a hydrogen peroxide-inducible catalase. J. Bacteriol. **178:** 6802–6809
110 Sigaud S., Becquet V., Frendo P., Puppo A. and Herouart D. (1999) Differential regulation of two divergent *Sinorhizobium meliloti* genes for HPII-like catalases during free-living growth and protective role of both catalases during symbiosis. J. Bacteriol. **181:** 2634–2639
111 Fondren L. M., Sloan G. L., LeBlanc P. A. and Heath H. E. (1994) Plasmid-encoded catalase of *Staphylococcus simulans biovar staphylolyticus*. FEMS Microbiol. Lett. **117:** 231–235
112 Horsburgh M. J., Ingham E. and Foster S. J. (2001) In *Staphylococcus aureus*, fur is an interactive regulator with PerR, contributes to virulence and is necessary for oxidative stress resistance through positive regulation of catalase and iron homeostasis. J. Bacteriol. **183:** 468–475
113 Hahn J. S., Oh S. Y., Chater K. F., Cho Y. H. and Roe J. H. (2000) $H_2O_2$-sensitive fur-like repressor CatR regulating the major catalase gene in *Streptomyces coelicolor*. J. Biol. Chem. **275:** 38254–38260.
114 Cho Y. H., Lee E. J. and Roe J. H. (2000) A developmentally regulated catalase required for proper differentiation and osmoprotection of *Streptomyces coelicolor*. Mol. Microbiol. **35:** 150–160
115 Hahn J. S., Oh S. Y. and Roe J. H. (2000) Regulation of the furA and catC operon, encoding a ferric uptake regulator homologue and catalase-peroxidase, respectively, in *Streptomyces coelicolor* A3(2). J. Bacteriol. **182:** 3767–3774
116 Zou P., Borovok I., Ortiz de Orue Lucana D., Muller D. and Schrempf H. (1999) The mycelium-associated *Streptomyces reticuli* catalase-peroxidase, its gene and regulation by FurS. Microbiology **145:** 549–559
117 Visick K. L. and Ruby E. G. (1998) The periplasmic, group III catalase of *Vibrio fischeri* is required for normal symbiotic competence and is induced both by oxidative stress and by approach to stationary phase. J. Bacteriol. **180:** 2087–2092
118 Mongkolsuk S., Loprasert S., Vattanaviboon P., Chanvanichayachai C., Chamnongpol S. and Supsamran N. (1996) Heterologous growth phase- and temperature-dependent expression and H2O2 toxicity protection of a superoxide-inducible monofunctional catalase gene from *Xanthomonas oryzae pv. oryzae*. J. Bacteriol. **178:** 3578–3584.
119 Vattanaviboon P. and Mongkolsuk S. (2000) Expression analysis and characterization of the mutant of a growth-phase- and starvation-regulated monofunctional catalase gene from *Xanthomonas campestris pv. phaseoli*. Gene **241:** 259–265
120 Evans S. (1993). SETOR: hardware lighted three-dimensional solid model representations of macromolecules. J. Mol. Graphics. **11:** 134–138
121 Kleywegt G. J. and Jones T. A. (1994). Detection, delineation, measurement and display of cavities in macromolecule structures. Acta Crystallog. D**50:** 178–185